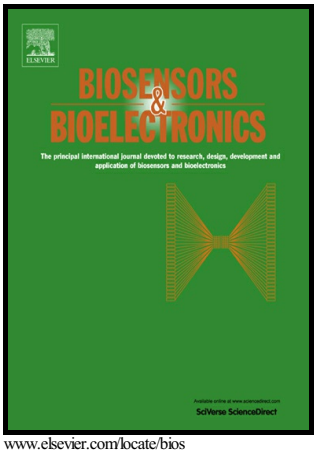

www.elsevier.com/locate/bios

Enzyme-assisted cycling amplification and DNA-templated *in-situ* deposition of silver nanoparticles for the sensitive electrochemical detection of Hg^{2+}

Hua Xie, Qin Wang, Yaqin Chai, Yali Yuan, Ruo Yuan

PII: S0956-5663(16)30664-9
DOI: http://dx.doi.org/10.1016/j.bios.2016.07.035
Reference: BIOS8916

To appear in: *Biosensors and Bioelectronic*

Received date: 30 January 2016
Revised date: 6 June 2016
Accepted date: 11 July 2016

Cite this article as: Hua Xie, Qin Wang, Yaqin Chai, Yali Yuan and Ruo Yuan, Enzyme-assisted cycling amplification and DNA-templated *in-situ* deposition o silver nanoparticles for the sensitive electrochemical detection of Hg^{2+} *Biosensors and Bioelectronic,* http://dx.doi.org/10.1016/j.bios.2016.07.035

Enzyme-assisted cycling amplification and DNA-templated *in-situ* deposition of silver nanoparticles for the sensitive electrochemical detection of Hg^{2+}

Hua Xie, Qin Wang, Yaqin Chai, Yali Yuan*, Ruo Yuan*

Key Laboratory of Luminescent and Real-Time Analytical Chemistry (Southwest University), Ministry of Education, College of Chemistry and Chemical Engineering, Southwest University, Chongqing 400715, PR China

Abstract:

In this work, a label-free electrochemical biosensor was developed for sensitive and selective detection of mercury (II) ions (Hg^{2+}) based on *in-situ* deposition of silver nanoparticles (AgNPs) on terminal deoxynucleotidyl transferase (TdT) extended ssDNA for signal output and nicking endonuclease for cycling amplification. In the presence of target Hg^{2+}, the T-rich DNA (HP1) could partly fold into duplex-like structure (termed as output DNA) *via* T-Hg^{2+}-T base pairs and thus exposed its sticky end. The sticky end of output DNA could then hybridize with 3′-PO_4 terminated capture DNA (HP2) on electrode surface to form output DNA-HP2 hybridization complex with the sequence 5′-CCTCAGC-3′/3′-GGAGTCG-5′ (the sequence could be recognized by nicking endonuclease Nt.BbvCI). With the introduction of Nt.BbvCI, output DNA existed in hybridization complex was released from electrode and participated in the next hybridization process, accompanying with

* Corresponding author. Tel.: +86-23-68252277; Fax: +86-23-68253172.

E-mail address: y198688@swu.edu.cn (YL. Yuan); yuanruo@swu.edu.cn (R. Yuan)

the cleave of HP2 to expose substantial 3′-OH group, which could be extended into a long ssDNA nanotail with the aid of TdT and deoxyadenosine triphosphate (dATP). Since the long negatively charged ssDNA nanotail absorbed the positively charged silver ions on the DNA skeleton, the metallic silver could be *in-situ* deposited on electrode surface for electrochemical signal output upon addition of reduction regent sodium borohydride. Under optimal conditions, the developed electrochemical biosensor presented a good response to Hg^{2+} with a detection limit of 3 pM (S/N = 3). Furthermore, the biosensor exhibited good reproducibility and high selectivity towards other interfering ions. The proposed sensing system also showed a promising potential application in real sample analysis.

Keywords: electrochemical biosensor, Hg^{2+}, nicking endonuclease, terminal deoxynucleotidyl transferase, metallic silver

1. Introduction

Mercury ion (Hg^{2+}) is one of the toxic heavy mental pollutants in the environment and can be accumulated in vital organs and tissues through the food chain, leading to various serious human diseases (Nolan and Lippard, 2008; Tchounwou et al., 2003; Harris et al., 2003; Afkhami et. al., 2012; Bagheri et. al, 2015). Therefore, the development of facile, sensitive, and reliable methods for efficient detection of Hg^{2+} is particularly essential and vital in environmental protection and disease prevention. Much effort has been made to develop the Hg^{2+} sensors, including electrochemical (Guo et al., 2011; Xu et al., 2015), electrochemiluminescence (Zhang et al., 2013; Huang et al., 2015), colorimetric (Li et

al., 2015; Ren et al., 2015), fluorescence (Zheng et al., 2013; Wang et al., 2014), surface-enhanced Raman scattering (Zhang et al., 2013) and so on. Among these biosensors, electrochemical biosensor based on the fact that thymine base pairs can selectively capture Hg^{2+} to form T-Hg^{2+}-T complex (Miyake et al., 2006) has captivated the attention of scientists due to the advantages of high sensitivity, excellent flexibility, fast response, simple instrumentation and low cost.

Recently, DNA nicking endonuclease has attracted tremendous interest in biological detection due to its strong recognition for DNA sequences (Xu et al., 2009). During nicking endonuclease cleavage process, the target or substance related with target can be reused through repeated cycles of hybridization, cleavage, and dissociation, resulting in an obvious amplification of the signal (Chen et al., 2010). To further improve the detection sensitivity of biological samples, the nicking endonuclease is usually combined with other amplification strategies, such as polymerase chain reaction (PCR) (Erlich et al., 1991), rolling circle amplification (RCA) (Ye et al., 2012), loop-mediated isothermal amplification (LAMP) (Xie et al., 2014), hybridization chain reaction (HCR) (Yao et al., 2015). Nevertheless, these strategies often require relatively long assay time, complicated preparation, specific equipment or the complex process of designing probes. In contrast, terminal deoxynucletidyl transferase (TdT), a template-independent DNA polymerase, could catalyze the sequential addition of deoxynucleotides (dNTPs) at the 3′-OH group of the DNA to produce a long single-stranded DNA (ssDNA) nanotail, thereby presenting a facile, direct, and cost-effective way for signal amplification (Shen et al.,

2015; Tjong et al., 2013). To the best of our knowledge, the electrochemical biosensor which combined nicking endonuclease with TdTase-mediated extension was relatively rare.

Silver nanoparticles (AgNPs) are known as an excellent electrochemical tag due to their lower oxidation potential with a relatively sharp peak (Lin et al., 2012). Usually, AgNPs are converted from silver ion (Ag^+) and DNA rich of phosphate groups has high affinity for positively charged Ag^+, thus these localized Ag^+ could be *in-situ* reduced to form metallic silver (Gao et al., 2013; Lin et al., 2011) under reduction regent. This process is selective and restricted to the DNA template only, which endows negatively charged DNA with possibility that acting as template for the fabrication of metallic and semi-conducting nanowires (Wu et al., 2014). Therefore, in this work, TdTase extended ssDNA was acted as template and the AgNPs were then formed on the DNA skeleton *via in situ* chemical reduction of electrostatically absorbed Ag^+ for electrochemical signal output.

Herein, a label-free electrochemical biosensor for sensitive Hg^{2+} detection was designed with *in-situ* deposition of AgNPs on TdT extended ssDNA for signal output and nicking endonuclease assisted cycling amplification. As shown in Scheme 1, the hairpin HP1 contained domain 1 of T-rich sequence and domain 2 of partially complementary to domain 1. And the hairpin HP2 had the nicking endonuclease Nt.BbvCI recognition sequence which was blocked by the hairpin stem region. In the presence of Hg^{2+}, HP1 would specifically combine with the target Hg^{2+} by the T-Hg^{2+}-T interaction to form output DNA, exposing its sticky end to hybridize with

the 3′-PO_4 terminated HP2 to form output DNA-HP2 hybridization complex, which contained a cleavage site of nicking endonuclease (Nt.BbvCI). With the aid of Nt.BbvCI, the cleavage sites of HP2 were cut and exposed substantial 3′-OH group. Simultaneously, output DNA was released from the hybridization complex to initiate recycling hybridization process, which resulted in generating a great deal of cleaved HP2 fragments with 3′-OH terminal. Since the 3′-OH group on the electrode surface could trigger sequential DNA extension in the presence of TdT and deoxyadenosine triphosphate (dATP), there would be substantial long ssDNA to absorb positively charged Ag^+ *via* electrostatic interaction. Then AgNPs were *in-situ* reduced on the electrode for electrochemical signal output which can be used to quantitatively measure the concentration of Hg^{2+}. This proposed strategy exhibited high sensitivity and excellent selectivity, providing a universal sensing platform for other targets.

(Scheme 1)

2. Experimental section

2.1 Chemicals and Materials

Chloroauric acid ($HAuCl_4$), trisodium citrate, silver nitrate ($AgNO_3$), sodium borohydride ($NaBH_4$), Tris(2-carboxyethy)phosphine hydrochloride (TCEP) and 6-mercaptohexanol (MCH) were purchased from Sigma (St. Louis, MO, USA). Nicking endonuclease (Nt.BbvCI) and 10×NEB buffer were purchased from New England Biolabs Ltd. (Beijing, China). Terminal deoxynucleotidyl transferase (TdT) and TdT buffer (1 M potassium cacodylate, 5 mM $CoCl_2$, 0.05% (*V/V*) Triton X-100 and 0.125 M Tris, pH 7.2 at 25 °C) were provided by Beyotime Biotechnology Co.

Ltd. (Nantong, China). Deoxyadenosine triphosphate (dATP) was obtained from Sangon Inc. (Shanghai, China). $K_3[Fe(CN)_6]$ and $K_4[Fe(CN)_6]$ were purchased from Beijing Chemical Reagent Co. (Beijing, China). Ultrapure water obtained from a Millipore water purification system (18.2 MΩ, MilliQ, Millipore) was used in all experiments. All DNA oligonucleotides were synthesized and purified by Sangon Biotech Co., Ltd. (Shanghai, China). The nucleotide sequences were listed as follows:

HP1: 5′-AATTG GGCTG AGGAT CGGGT GA**CCC AATTC TTTCC CCTTT GTTTT GGG**-3′

HP2: 5′-SH-$(CH_2)_6$-ACTGT AATTG GGATC CGATC C↓TCAG CCCAA TT-PO_4-3′

HP1 contained T-rich sequence which was expressed as bold, HP2: the recognition sequence of Nt.BbvCI was expressed as single underline and the downward facing arrows showed the nicking site of nicking enzyme. The buffers involved in this work were prepared as follows: 10 mM Tris-HCl, 1.0 mM EDTA, 10 mM TCEP, 0.1 M NaCl (pH 7.4) was used as immobilization buffer; 20 mM Tris-HCl, 50 mM $MgCl_2$ (pH 7.4) was used for dissolving oligonucleotide HP1; 0.1 M phosphate buffered solutions (PBS, pH 7.0) containing 0.1 M Na_2HPO_4, 0.1 M NaH_2PO_4, and 0.1 M $MgCl_2$ was served as working buffer to perform electrochemical measurements.

2.2. Apparatus and Measurements

Cyclic voltammetry (CV), electrochemical impedance spectroscopy (EIS) and differential pulse voltammetry (DPV) were performed on a CHI 660D electrochemical workstation (Shanghai Chen Hua Instrument, Shanghai, China). A

traditional three electrode system consisted of a platinum wire as the auxiliary electrode, a saturated calomel electrode (SCE) as the reference electrode and a bare or modified glassy carbon electrode (GCE, Φ = 4 mm) as the working electrode. The pH measurements were performed on a pH meter (MP 230, Mettler-Toledo, Switzerland). The morphological characterization of fabricated electrode was performed by atomic force microscopy (AFM, Vecco, USA).

2.3. Electrochemical measurements

CV of the electrode fabrication was performed in 2 mL 5.0 mM $[Fe(CN)_6]^{3-/4-}$ solution, scanning from -0.2 V to 0.6 V at a scan rate of 100 $mV \cdot s^{-1}$. EIS was carried out in 2 mL $[Fe(CN)_6]^{3-/4-}$ solution (5.0 mM) containing 0.1 M KCl with the frequencies swept from 0.1 to 10^5 Hz. DPV measurements were taken in 2 mL PBS (pH 7.0) with the potential ranging from 0 to 0.2 V, the modulation amplitude of 0.05 V, the pulse width of 0.05 s and the sample width of 0.0167 s.

2.4. Fabrication of electrochemical biosensor

Prior to use, HP1 and HP2 were heated to 95 °C for 5 min and then slowly cooled to room temperature to form stem-loop structure. First of all, the GCE was carefully polished with 0.3 and 0.05 μm alumina slurries to obtain a mirror-like surface and successively ultrasonicing in ultrapure water, ethanol, and ultrapure water. The pretreated GCE was immersed into $HAuCl_4$ solution for electrodeposition under constant potential of -0.2 V for 30 s to obtain deposition AuNPs (depAu) layer. Next, 20 μL of 2 μM thiol-modified HP2 was attached onto the depAu layer for 16 h at room temperature *via* Au-S affinity. After washing by ultrapure water, the electrode

was treated with 1.0 mM MCH for 30 min. Meanwhile, 2 μM HP1 incubated with various concentrations of Hg^{2+} at room temperature for 1 h. Subsequently, 20 μL mixture containing 17.5 μL above solution (HP1 and Hg^{2+}) and 0.5 μL Nt.BbvCI (10000 $U \cdot mL^{-1}$) and 2 μL 10×NEB buffer was dripped onto the modified electrode and incubated for 60 min at 37 °C to generate numerous HP2 fragment with 3′-OH group. After rinsing with ultrapure water, the electrode was immersed in TdT extension solution (200 $U \cdot mL^{-1}$ TdT and 4 mM dATP) and incubated at 37 °C for 60 min to form long ssDNA nanotail. Then, 10 μL of $AgNO_3$ solution (50 μM) was dropped on the electrode surface for 30 min in the dark. Subsequently, 10 μL freshly prepared $NaBH_4$ (1 mM) in citrate buffer was carefully added to the electrode surface and incubated for 30 min in the dark to obtain AgNPs on the DNA skeleton. Finally, the electrode was washed with ultrapure water, and then electrochemical measurements were performed.

2.5. Preparation of rice sample

Rice sample was immersed in 0.1 mM Hg^{2+} for a week. Then the contaminated rice was washed with water three times, dried and ground into power. Next, 1.0 g sample was digested with 10 mL of 5 M nitric acid (HNO_3) and boiled to almost dryness (~1 mL left). After adding 3 mL of water, the mixture was filtered through a membrane filter of 0.2 μm pore size and the filtrate was centrifugated at 12000 rpm for 15 min. Finally, the supernatant was diluted with water to a total volume of 10 mL and adjusted the pH to 7.0 with NaOH.

3. Results and discussion

3.1. The characterization of the stepwise modified electrode

The modification process of electrode surface was monitored by CV. Fig. 1A showed the voltammograms of the electrode modification in 5.0 mM $[Fe(CN)_6]^{3-/4-}$ solution. The bare GCE exhibited a couple of quasi-reversible redox peak (curve a). After electrodepositing AuNPs (depAu) onto the electrode, an obviously raised peak current was obtained (curve b), indicating that depAu had excellent conductive property and could greatly promote the electron transfer. After assembling of HP2 onto electrode, an obvious decreased peak current (curve c) was achieved, demonstrating the successful modification of HP2. After nonconductive MCH was applied to block non-specific sites, a successive decline of peak current was detected (curve d). Followed by incubating with Nt.BbvCI (10000 $U \cdot mL^{-1}$) and output DNA, the peak current increased apparently (curve e), accounting for the fact that the cleavage sites of HP2 were cut and dissociated from electrode surface, then the repulsion effect reduced between negatively charged HP2 and negatively charged $[Fe(CN)_6]^{3-/4-}$. As expected, the current response was obviously reduced (curve f) after TdTase-mediated extension, due to the introduction of more negative charges on the electrode surface upon formation of the long ssDNA. These results demonstrated that the proposed electrochemical biosensor was successfully fabricated.

EIS has been proved to be one of the most powerful tools for interfacial investigation (Bardea, et al., 1999; Giroud, et al., 2009), we used this technique to confirm the fabrication process of the electrochemical biosensor. Fig. 1B displayed the impedance spectra of the modified electrode at different step in the presence of 5

mM $[Fe(CN)_6]^{3-/4-}$ solution containing 0.1 M KCl. The bare GCE exhibited a small semicircle (curve a), indicating a relatively low resistance. After modification of depAu on the GCE, a decreased semicircle was observed (curve b) owing to the excellent conductivity of depAu. However, with the successive immobilization of negatively charged HP2 and nonconductive MCH, the resistance sequentially increased (curve c and d). After the modified electrode was treated with Nt.BbvCI (10000 $U \cdot mL^{-1}$) and output DNA, the resistance was decreased again (curve e), which was attributed to the fact that considerable HP2 strands were cut and dissociated from electrode surface. The resistance was increased (curve f) after TdTase-mediated extension, this was caused by the formed long ssDNA on the electrode which increased the effect of steric hindrance and decreased the electron-transfer efficiency. These results were in good accordance with that observed in CV (Fig. 1A), indicating the successful fabrication of the electrochemical biosensor.

In addition, AFM was further employed to investigate the fabrication process of the proposed electrochemical biosensor. Fig. S1 showed a significant change of the surface morphology after each modified step. Fig. S1A showed an image of depAu on the electrode, which displayed spherical particles. After incubated with HP2 onto the electrode, the films gradually became rough (Fig. S1B). When subsequent assembly with MCH and mixture containing HP1, Hg^{2+} and Nt.BbvCI (10000 $U \cdot mL^{-1}$), more rough films could be observed (Fig. S1C and D). After extension by TdTase, surface morphology of the modified films was changed obviously (Fig. S1E). These results also validated that the proposed electrochemical biosensor was successfully

fabricated.

(Fig. 1)

3.2. The signal amplification of Nt.BbvCI and TdTase-mediated extension

To estimate the signal amplification function of the proposed biosensor, DPV responses of different modified electrodes which were treated with $AgNO_3$ and $NaBH_4$ were recorded. As shown in Fig. 2, in the absence of Hg^{2+}, the conformation of HP1 kept unchanged, and there was no output DNA to hybridize with HP2. Thus, a small current response (curve a) was obtained due to a little amount of Ag^+ absorbed on the HP2. In the presence of 10 nM Hg^{2+} (without Nt.BbvCI and TdTase-mediated extension), Hg^{2+} combined with HP1 to produce output DNA, which could further hybridize with HP2. And there was HP2 and output DNA-HP2 hybridization complex on the electrode surface, causing enhanced adsorbed Ag^+ amount. Therefore, the current response increased (curve b) compared with that of curve a. However, after the addition of Nt.BbvCI, the current response decreased (curve c). It was ascribed to the fact that the HP2 in output DNA-HP2 hybridization complex was cleaved. Simultaneously, output DNA was released from the hybridization complex and could be used to hybridize with other HP2, starting a new cycle of hybridization process. Finally, there was few HP2 and amounts of cleaved HP2 fragment on the electrode surface, resulting in decreased absorption amount of Ag^+. After Nt.BbvCI cleavage process and TdTase-mediated extension occurred, a very strong current peak (curve d) was observed, which was due to the fact that long ssDNA absorbed large amount of Ag^+, and thus *in-situ* produced substantial AgNPs on the electrode, causing the

enhanced electrochemical signal output. The experimental results clearly indicated that the combined employment of Nt.BbvCI-assisted cycling and TdTase-mediated extension could amplify the signal significantly.

(Fig. 2)

3.3. Optimization of the experimental conditions

In order to achieve optimal sensing performance, the important experimental parameters such as TdTase-mediated extension reaction time and the concentration of $AgNO_3$ were investigated by electrochemical biosensor with 10 nM Hg^{2+}. With the elongation of the enzyme reaction time, more substrates of dATP can be incorporated into the DNA and the length of ssDNA increased, which arose an increased amount of Ag^+. As shown in Fig. 3A, response currents gradually increased accompanying with the elongation of the enzyme reaction time spanned from 15 min to 60 min, and then reached a plateau at 60 min. This might be the fact that sufficient dATP meet the requirement of high-efficient catalytic addition by TdT in the primary reaction period. With the ongoing excessive exhaustion of dATP, the reaction efficiency gradually declined. Therefore, 60 min was chosen the optimal enzymatic reaction time for the incorporation of dATP into extended DNA chain.

The concentration of $AgNO_3$ also had significant influence on the electrochemical biosensor, because the response current of the biosensor depended on the absorption amount of Ag^+ on the DNA skeleton. As shown in Fig. 3B, the peak current rapidly increased with augment of incubation concentration of $AgNO_3$ from 10 μM to 50 μM and then leveled off after over 50 μM. Therefore, the optimal $AgNO_3$

concentration of 50 μM was applied in this experiment.

(Fig. 3)

3.4. Electrochemical assay of Hg^{2+}

Under the optimal experimental conditions, the proposed electrochemical biosensor was applied to detect different concentrations of Hg^{2+}. Fig. 4A displayed the DPV dynamic responses corresponding to various concentrations of Hg^{2+}. It was clearly shown that the peak current increased with the augment of Hg^{2+} concentration. As shown in Fig. 4B, peak current was proportional to the logarithm value of Hg^{2+} in the range from 0.01 nM to 100 nM and the regression equation was $I = 4.795 \lg c + 17.440$ with a correlation coefficient of 0.9984, where I and c represented the peak current intensity and Hg^{2+} concentration, respectively. The detection limit was calculated to be 3 pM at a signal-to-noise ratio of 3.

In addition, the analytical performance of the proposed method was compared with other reported Hg^{2+} detection methods. As shown in Table 1, our detection method had a satisfactory linear range and a relatively low detection limit and the detection limit of the proposed electrochemical biosensor was lower than above detection methods. These results further indicated that the proposed electrochemical biosensor was reliable and sensitive for quantitative determination of Hg^{2+}, which was attributed to the employment of Nt.BbvCI-assisted cycling and TdT extended ssDNA to absorb a great deal of Ag^{+}, significantly amplifying the electrochemical signal.

(Fig. 4.)

3.5. Selectivity and reproducibility of the electrochemical biosensor

To assess the selectivity and specificity of the proposed electrochemical biosensor, interfering metal ions including Mn^{2+}, Pb^{2+}, Ni^{2+}, Cd^{2+}, Fe^{3+}, Cu^{2+}, Zn^{2+} (1 μM, respectively) were investigated under the same conditions. As shown in Fig. 5, it was obvious that when interfering metal ions were incubated alone, the DPV responses were almost the same as that of the blank sample. However, when 10 nM Hg^{2+} was coexisted with the interfering metal ions, no significant changes were observed compared to the Hg^{2+} existed alone. Corresponding DPV curves of interfering metal ions were displayed in Fig. S3. The satisfactory results indicated that developed biosensor had good selectivity to the Hg^{2+} detection, which could ascribe to the fact that T-T mismatch bases had high affinity for Hg^{2+} against many other metal ions.

The reproducibility of the electrochemical biosensor was investigated by analyzing the same concentration of Hg^{2+} (10 nM) with intra- and inter-assay for four times. The relative standard deviation (RSD) of intra- and inter-assays were 2.5% and 4.9%, respectively. These results showed the proposed biosensor possessed good precision and acceptable reproducibility.

(Fig. 5)

3.6. Real sample analysis

To validate the practical application of our proposed method, we tested the recovery experiments with the standard addition method in river water (collected from Jialing River, China). The results were summarized in Table 2, satisfactory recovery values (91.5%-108.8%) were obtained. Additionally, we determined the concentration

of Hg^{2+} in the contaminated rice sample, which was estimated to be 4.56 ± 0.13 nM. Therefore, the proposed electrochemical biosensor could successfully apply to Hg^{2+} analysis in real environmental sample and food sample.

4. Conclusions

In summary, a label-free electrochemical biosensor based on *in-situ* deposition of AgNPs on TdT extended ssDNA for signal output and nicking endonuclease assisted cycling amplification had been designed for Hg^{2+} detection in this paper. The wide linear range and low detection limit of the proposed biosensor should be attributed to the following reasons. Firstly, nicking endonuclease Nt.BbvCI was applied to initiate recycling to generate a large number of cleaved HP2 fragments with 3′-OH terminal, which then was acted as the primer of the TdTase-mediated extension for realizing the absorption of numerous Ag^{+}, thus inducing significant enhancement of the electrochemical signal. Secondly, DNA-template deposition of AgNPs was acted as an effective electrochemical signal tag, avoiding the sophisticated labeling steps and the need of silver enhancement substrates. Thirdly, high specificity of T-T mismatch bases to the Hg^{2+} greatly improved the selectivity. The successful implementation of Nt.BbvCI-assisted cycling and TdTase-mediated DNA extension remarkably amplified the electrochemical signal and improved the sensitivity of the analytical method. For these advantages, the proposed strategy held good potential for sensitive determination of other targets in future.

Acknowledgements

This work was financially supported by the NNSF of China (51473136,

21575116, 21505107), the Fundamental Research Funds for the Central Universities (XDJK2014C138, SWU115037), and Chongqing Graduate Research Innovation Project Foundation (CYS2015057).

References

Afkhami, A., Bagheri, H., Khoshsafar, H., Saber-Tehrani, M., Tabatabaee, M., Shirzadmehr, A., 2012. Anal. Chim. Acta 746, 98-106.

Bagheri, H., Afkhami, A., Khoshsafar, H., Rezaei, M., Sabounchei, S.J., Sarlakifar, M., 2015. Anal. Chim. Acta 870, 56-66.

Bardea, A., Patolsky, F., Dagan, A., Willner, I., 1999. Chem. Commun. 21, 21-22.

Chen, J., Zhang, J., Li, J., Fu, F., Yang, H.H., Chen, G., 2010. Chem. Commun. 46, 5939-5941.

Erlich, H.A., Gelfand, D., Sninsky. J.J., 1991. Science 252, 1643-1651.

Gao, F.L., Lei, J.P., Ju, H.X., 2013. Anal. Chem. 85, 11788-11793.

Giroud, F., Gorgy, K., Gondran, C., Cosnier, S., Pinacho, D.G., Marco, M.P., Sánchez-Baeza, F.J., 2009. Anal. Chem. 81, 8405-8409.

Guo, L.Q., Yin, N., Nie, D.D., Fu, F.F., Chen. G.N., 2011. Chem. Commun. 47, 10665-10667.

Harris, H.H., Pickering, I.J., George, G.N., 2003. Science 301, 1203.

Huang, R.F., Liu, H.X., Gai, Q.Q., Liu, G.J., Wei, Z., 2015. Biosens. Bioelectron. 71, 194-199.

Li, W., Chen, B., Zhang, H.X., Sun, Y.H., Wang, J., Zhang, J. L., Fu, Y., 2015. Biosens. Bioelectron. 66, 251-258.

Lin, D.J., Wu, J., Wang, M., Yan, F., Ju, H.X., 2012. Anal. Chem. 84, 3662-3668.

Lin, Y.H., Yin, M.L., Pu, F., Ren, J.S., Qu, X.G., 2011. Small 7, 1557-1561.

Miyake, Y., Togashi, H., Tashiro, M., Yamaguchi, H., Oda, S., Kudo, M., Tanaka, Y., Kondo, Y., Sawa, R., Fujimoto, T., Machinami, T., Ono, A., 2006. J. Am. Chem. Soc. 128, 2172-2173.

Nolan, E.M., Lippard, S.J., 2008. Chem. Rev. 108, 3443-3480.

Ren, W., Zhang, Y., Huang, W.T, Li, N.B., Luo, H.Q., 2015. Biosens. Bioelectron. 68, 266-271.

Shen, Q.M., Han, L., Fan, G.C., Zhang, J.R., Jiang, L.P., Zhu, J.J., 2015. Anal. Chem. 87, 4949-4956.

Tchounwou, P.B., Ayensu, W.K., Ninashvili, N., Sutton. D., 2003. Environ. Toxicol. 18, 149-175.

Tjong, V., Yu, H., Hucknall, A., Chilkoti, A., 2013. Anal. Chem. 85, 426-433.

Wang, G., Xu, G., Zhu, Y., Zhang, X., 2014. Chem. Commun. 50, 747-750.

Wu, L., Wang, J.S., Ren, J.S., Qu, X.G., 2014. Adv. Funct. Mater. 24, 2727-2733.

Xie, S.B., Chai, Y.Q., Yuan, Y.L., Bai, L.J., Yuan, R., 2014. Biosens. Bioelectron. 55, 324-329.

Xu, H.F., Zhu, X., Ye, H.Z., Yu, L.S. Chen, G.N., Chi, Y.W., Liu, X.X., 2015. Chem. Commun. 51, 15031-15034.

Xu, W., Xue, X., Li, T., Zeng, H., Liu, X., 2009. Angew. Chem. Int. Ed. 48, 6849-6852.

Yao, G.H., Liang, R.P., Yu, X.D., Huang, C.F., Zhang, L., Qiu, J.D., 2015. Anal. Chem.

87, 929-936.

Ye, S.J., Yang, Y.X., Xiao, J., Zhang, S.S., 2012, Chem. Commun. 48, 8535-8537.

Zhang, L., Chang, H.X., Hirata, A., Wu, H.K., Xue, Q.K., Chen, M.W., 2013. ACS Nano. 7, 4595-4600.

Zhang, L.L., Wong, J.X.H., Li, X.C., Li, Y.C., Yu, H.Z., 2015. Anal. Chem. 87, 5062-5067.

Zhang, M., Ge, L., Ge, S., Yan, M., Yu, J., Huang, J., Liu, S., 2013. Biosens. Bioelectron. 41, 544-550.

Zheng, J., Nie, Y.H., Hu, Y.P., Li, J.S., Li, Y.H., Jiang, Y., Yang, R.H., 2013. Chem. Commun. 49, 6915-6917.

Scheme 1. Schematic illustration of the electrochemical biosensor for Hg^{2+} detection based on *in-situ* deposition of AgNPs on TdT extended ssDNA for signal output and nicking endonuclease assisted cycling amplification.

Fig. 1. CVs (A) and EIS (B) of the bare GCE (a), depAu/GCE (b), HP2/depAu/GCE (c), MCH/HP2/depAu/GCE (d), d incubated with 2 μM HP1 containing 10 nM Hg^{2+} and 10000 $U \cdot mL^{-1}$ Nt.BbvCI (e), e incubated with TdT and dATP (f) in 2 mL $[Fe(CN)_6]^{3-/4-}$ solution (5.0 mM, pH 7.4).

Fig. 2. The DPV responses of 2 μM HP1 with HP2 modified electrode in (a) absence of and (b) presence of 10 nM Hg^{2+}, (c) presence of 10 nM Hg^{2+} with Nt.BbvCI-assisted cycling, and (d) presence of 10 nM Hg^{2+} with Nt.BbvCI-assisted cycling and TdTase-mediated extension (10000 $U \cdot mL^{-1}$ Nt.BbvCI, 200 $U \cdot mL^{-1}$ TdT, 4 mM dATP, 60 min).

Fig. 3. The optimization of experimental parameters. (A) Influence of the time of TdTase-mediated extension reaction (200 $U \cdot mL^{-1}$ TdT, 4 mM dATP), the insert shows the dependence of peak currents on each incubation time. (B) Effect of the concentration of $AgNO_3$, the insert shows the dependence of peak currents on each concentration of $AgNO_3$ (error bars: SD, n = 3).

Fig. 4. (A) DPV responses of the electrochemical biosensor incubated with different concentrations of Hg^{2+} in 0.1 M PBS (pH 7.0). (B) The calibration plots of DPV peak current versus the logarithm of Hg^{2+} concentration (error bars: SD, n = 3).

Fig. 5. Selectivity of the electrochemical biosensor. The concentrations of interfering metal ions were 1 μM. The mixture contained 10 nM Hg^{2+} and 1 μM of other interfering metal ions, n = 3.

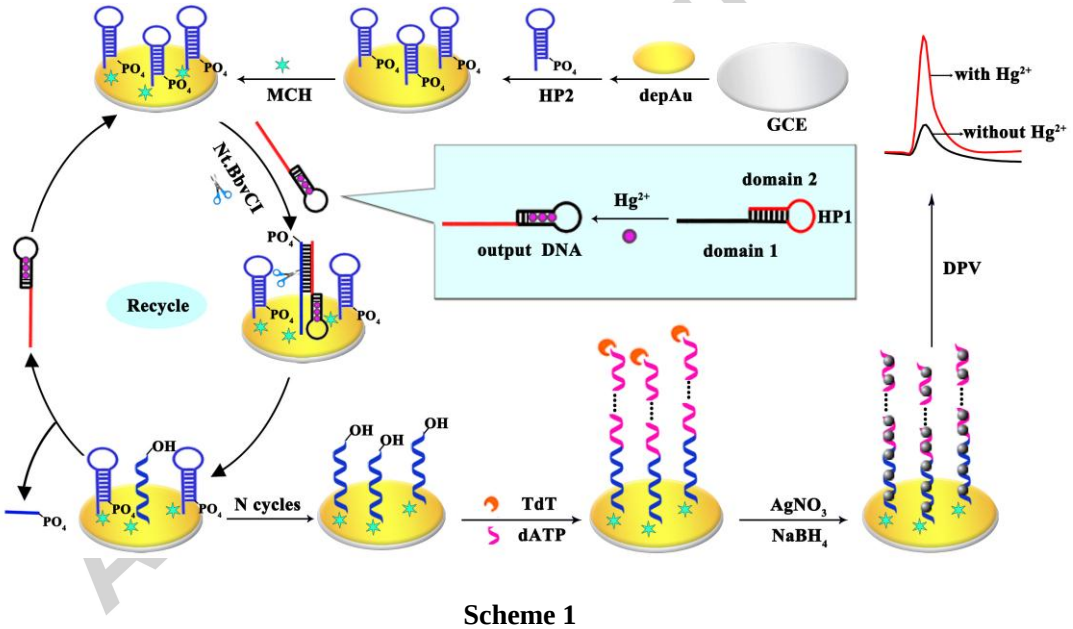

Scheme 1

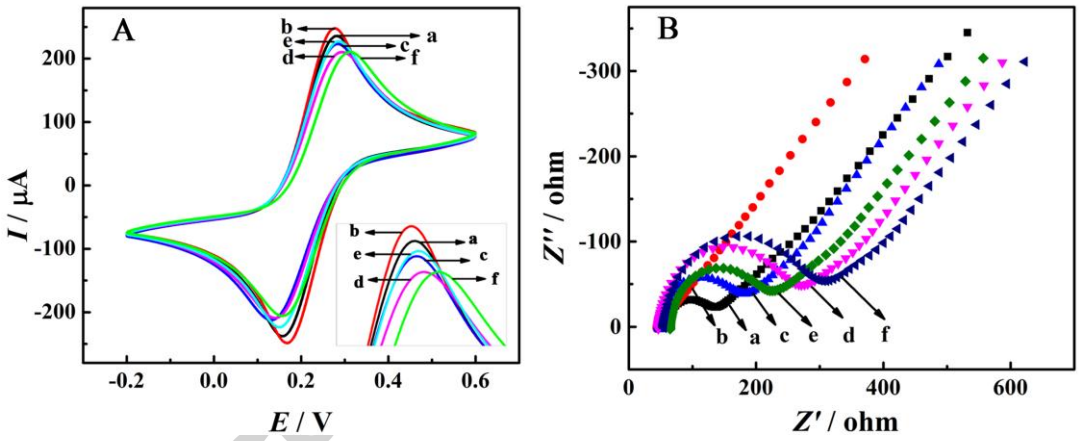

Fig. 1

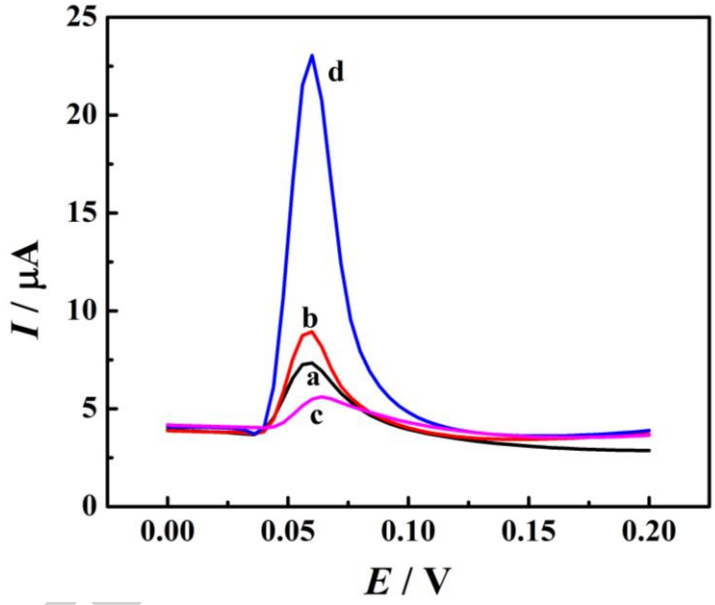

Fig. 2

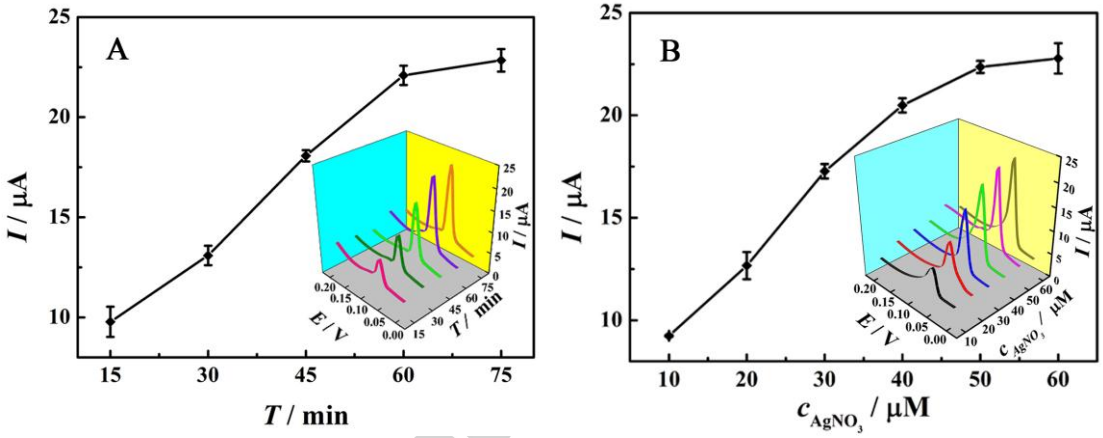

Fig. 3

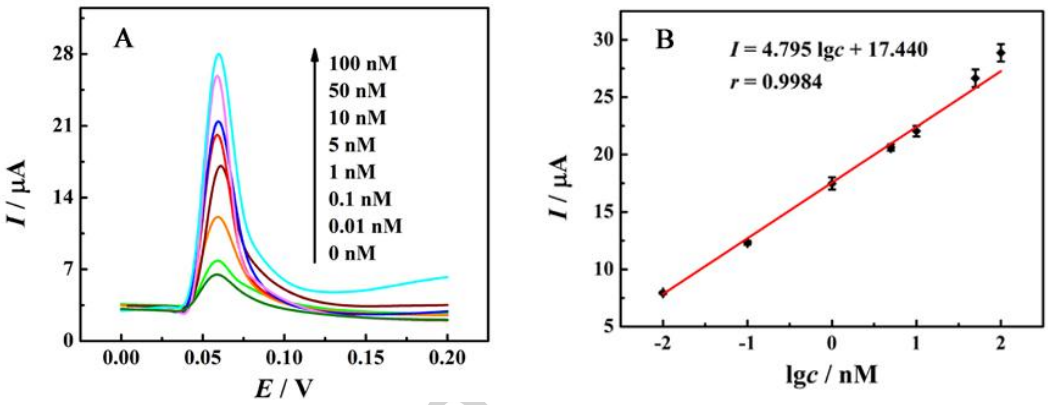

Fig. 4

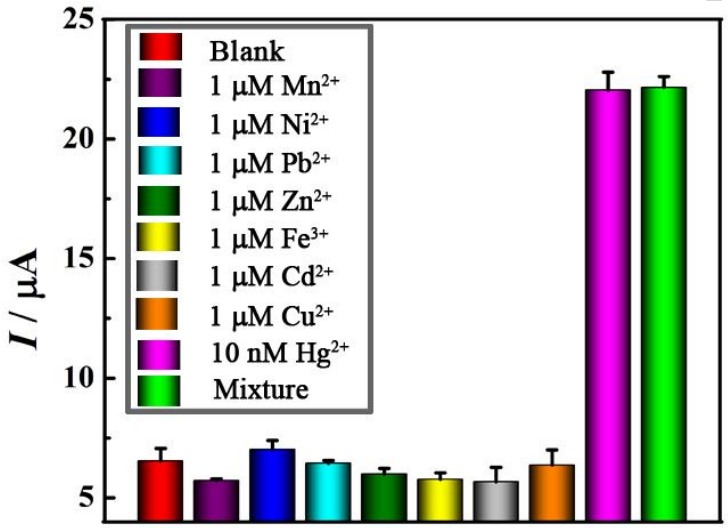

Fig. 5

Table 1. The proposed method compared with other Hg^{2+} analytical methods.

Analytical methods	Detection limit	Linear range	Ref
FL	0.3 nM	0.3-100 nM	Huang et al., 2014
ECL	0.3 nM	1-5000 nM	Cai et al., 2015
Colorimetric	0.125 nM	0.5-800 nM	Sun et al., 2014
SWV	5 pM	0.015-500 nM	Shi et al., 2014
DPV	5 nM	8-100 nM	Zhang et al., 2013
DPV	3 pM	0.01-100 nM	This work

Abbrevations: Fluorescence (FL); Electrochemiluminescence (ECL); Square wave voltammetry (SWV); Differential pulse voltammetry (DPV)

Table 2. Determination of Hg^{2+} in river water (n = 3) by the proposed electrochemical biosensor.

Sample number	**Concentration of Hg^{2+} Added/nM**	**Concentration of Hg^{2+} Found/nM**	**Recovery/%**	**RSD/%**
1	0.010	0.01059	105.9	5.7
2	0.10	0.1088	108.8	6.8
3	1.0	0.9725	97.3	9.1
4	5.0	4.574	91.5	7.7

References:

Cai, F.D., Zhu, Q., Zhao, K., Deng, A.P., Li. J.G., 2015. Environ. Sci. Technol. 49, 5013-5020.

Huang, J.H., Gao, X., Jia, J.J., Kim, J.K., Li, Z.G., 2014. Anal. Chem. 86, 3209-3215.

Shi, L., Chu, Z.Y., Liu, Y., Jin, W.Q., Chen, X.J., 2014. Biosens. Bioelectron. 54, 165-170.

Sun, Z.Z., Zhang, N., Si, Y.M., Li, S., Wen, J.W., Zhu, X.B., Wang, H., 2014. Chem. Commun. 50, 9196-9199.

Zhang, Y., Zhao, H., Wu, Z.J., Xue, Y., Zhang, X.F., He, Y.J., Li, X.J., Yuan, Z.B., 2013. Biosens. Bioelectron. 48, 180-187.

High Lights:

- DNA-template deposition of AgNPs was acted as an effective electrochemical signal tag.
- Nt.BbvCI-assited cycling and TdTase-mediated DNA extension amplified the electrochemical signal.
- The electrochemical biosensor exhibited excellent sensitivity, good selectivity, and acceptable reproducibility.